

*SUPPORTING INFORMATION*

Small angle neutron scattering contrast variation reveals  
heterogeneities of interactions in protein gels

A. Banc<sup>1</sup>, C. Charbonneau<sup>1</sup>, M. Dahesh<sup>1,2</sup>, M-S Appavou<sup>3</sup>, Z. Fu<sup>3</sup>, M-H. Morel<sup>2</sup>,  
L. Ramos<sup>1</sup>

<sup>1</sup> *Laboratoire Charles Coulomb (L2C), UMR 5221 CNRS-Université de Montpellier, F-34095  
Montpellier, France*

<sup>2</sup> *UMR IATE, UM-CIRAD-INRA-SupAgro, 2 pl Pierre Viala, 34070 Montpellier, France.*

<sup>3</sup> *Jülich Centre for Neutron Science JCNS, Forschungszentrum Jülich, Outstation at MLZ, D-85747  
Garching, Germany*

## **1. Protein extract composition**

The protein composition of the gluten protein extract was assessed by size exclusion high performance liquid chromatography (SE-HPLC) and reduced SDS-PAGE analysis. The respective proportions in glutenin polymer,  $\omega$ -gliadin,  $\gamma$ -gliadin,  $\alpha/\beta$ -gliadins, and chloroform/methanol soluble (CM) proteins (which are essentially albumin and globulin, alb/glo) were estimated from the differential integration of the SE-HPLC profile of the protein extract according to Morel et al<sup>1</sup> (see figure S1).

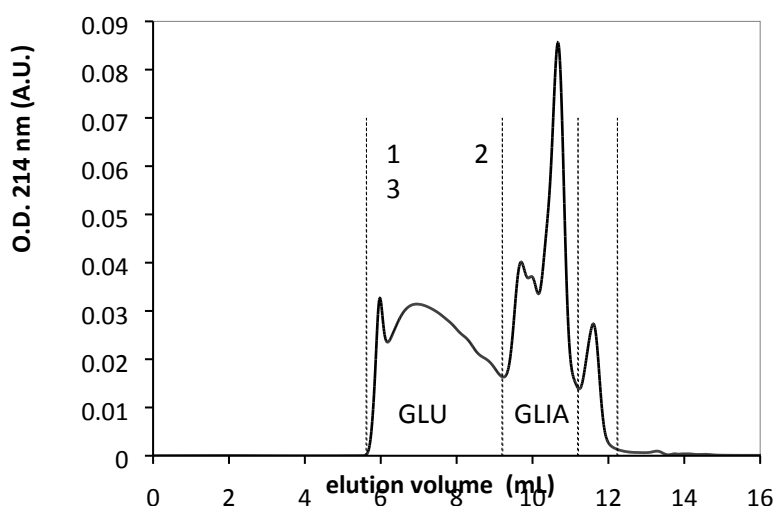


**Figure S1.** SE-HPLC profile of the wheat gluten protein fraction. The protein was dispersed in a 1% sodium-dodecyl-sulfate phosphate buffer, 20 $\mu$ L of the dispersion was injected on a TSK gel 4000SWXL (30 cm x 7.8 mm, 450 Å) and eluted at 0.7 ml.min<sup>-1</sup>. The first fraction (GLU) contains glutenin polymers (100 000 < Mw < 2.10<sup>6</sup> g/mol), the second fraction contains gliadins (GLIA; 25 000 < Mw < 100 000 g/mol) and the third fraction contains small Mw proteins (<25 000 g/mol). Fractions 1, 2 and 3 account respectively for 49, 43 and 8% of total protein.

The composition of the glutenin polymer in its  $x$  and  $y$  high-molecular-weight glutenin subunits types (HMW-GS), and their proportion in total protein were obtained from the densitometric analysis of the reduced protein SDS-PAGE pattern as shown in figure S2.

The proportion in low-molecular weight glutenin subunits (LMW-GS) in glutenin polymers was deduced by difference from the known proportions of high-molecular weight glutenin subunit (HMW-GS) (from SDS-PAGE) and glutenin polymers (from SE-HPLC). Similarly gliadins were distinguished into  $\omega$ -gliadin and  $\gamma$ -gliadin or  $\alpha/\beta$ -gliadin taking into consideration the results of SE-HPLC and SDS-PAGE analyses. The resulting composition of the gluten protein extract is given in table 1.

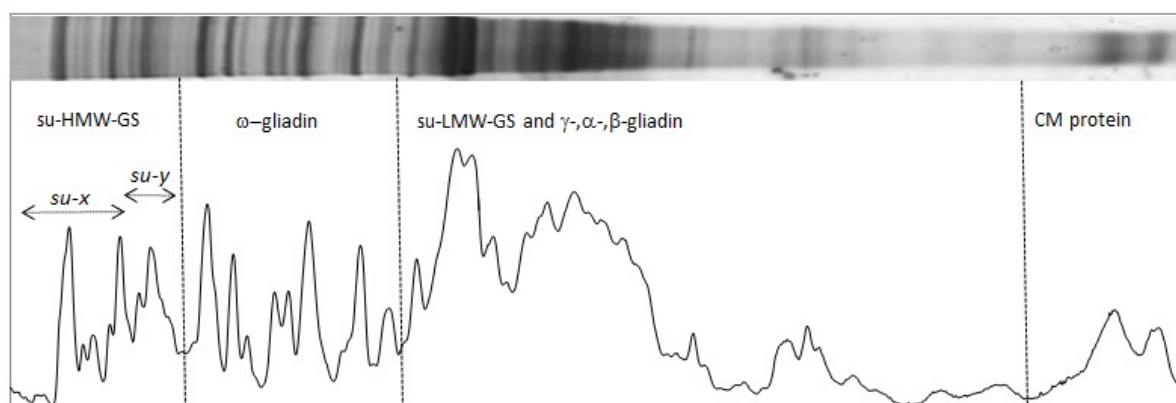


**Figure S2.** Densitometric profile of the SDS-PAGE pattern of the wheat gluten protein fraction. Proteins were reduced with 10 mM dithioerythriol and fractionated on a 12% SDS-PAGE prepared according to Laemmli's standard protocol. From the top (left) to the bottom of the gel: high-molecular-weight glutenin subunits of  $x$  and  $y$  types,  $\omega$ -gliadins, mixture of  $\gamma$ -,  $\alpha/\beta$ -gliadins and low-molecular-weight glutenin subunits. The last doublet consists in chloroform/methanol soluble (CM) proteins belonging to the class of  $\alpha$ -amylase/trypsin inhibitors<sup>2</sup>.

Composition of the wheat gluten protein extract					
glutenin polymers			gliadin		alb/glo
HMW-GS $x$	HMW-GS $y$	LMW-GS	$\omega$ -gliadin	$\gamma$ , $\alpha/\beta$ gliadin	CM protein
7%	6%	36%	20%	23%	8%

**Table 1.** Composition (in percent of total protein) of the wheat gluten protein extract as deduced from SE-HPLC and SDS-PAGE analyses.

## 2. Calculation of the average SLD of the protein extract

For the calculation of the average scattering length density (SLD) of the gluten protein extract, mean SLD values of the different wheat protein classes, namely HMW-GS type  $x$  and  $y$ , LMW-GS,  $\omega$ -,  $\gamma$ -,  $\alpha/\beta$ - gliadins and CM protein, were considered since industrial gluten is commonly obtained from a blend of different cultivars. The Jacrot<sup>3</sup> protonated amino-acid

SLD values were used to calculate mean SLD from the known amino-acid composition of typical wheat protein. Table II presents the mean SLD values and their standard deviations calculated considering at least three representative proteins of each class.

	SLD of wheat protein classes ( $10^{-6} \text{ \AA}^{-2}$ )						
	glutenin polymers			gliadin			alb/glo
	HMW-GSx <sup>a</sup>	HMW-GSy <sup>b</sup>	LMW-GS <sup>c</sup>	$\omega$ -gliadin <sup>d</sup>	$\gamma$ -gliadin <sup>e</sup>	$\alpha/\beta$ -gliadin <sup>f</sup>	CM protein <sup>g</sup>
<b>Protonated</b>	2.18 (0.01)	2.16 (0.01)	1.93 (0.04)	2.05 (0.05)	1.98 (0.04)	1.98 (0.02)	1.84 (0.03)
<b>Deuterated</b>	3.75 (0.04)	3.73 (0.04)	3.32 (0.07)	3.35 (0.13)	3.27 (0.07)	3.35 (0.03)	3.2 (0.2)

The following UniProtKB accession were considered for calculation. Standard deviation in brackets.

<sup>a</sup>P10388, P08489, Q1KL95, Q59910, Q6UKZ5, H9B854, Q0Q5D8.

<sup>b</sup>P08488, Q0Q5D8, A9ZMG8.

<sup>c</sup>Q8W3V2, P10386, P16315, Q8W3V5, Q00M61, Q6SPZ1, Q5MFQ2, Q6SPY7, B2BZD1, B2Y2R3, Q8W3X2.

<sup>d</sup>C0KEI0, Q571R2, R9XWH8, A0A060N0S6, C0KEI1, C0KEH9, A0A0B5J8A9, A0A0B5JD20, A0A0B5JHW1.

<sup>e</sup>P08079, P08453, P06659, P21292, P04729, P04730, M9TK56, R9XUS6.

<sup>f</sup>P18573, P04724, P04723, P02863, P04721, P04722, P04725, H6VLP5, A5JSA4.

<sup>g</sup>P93594, P16159, A8ROD1, A9JPD1, P30110.

**Table 2.** SLD of the different peptide classes identified in the wheat gluten fraction. Values for fully protonated proteins and values for proteins with 100% of exchangeable hydrogen replaced by deuterium are indicated.

The mean SLD value of the gluten protein extract calculated from the contribution of each protein classes (Table 1) and their individual SLD values (Table 2) is  $(1.99 \pm 0.14) 10^{-6} \text{ \AA}^{-2}$ . The standard deviation ( $0.14 10^{-6} \text{ \AA}^{-2}$ ) takes into account the standard deviation on the SLD of each class of protein but also a 5% uncertainty on their specific contribution to the total protein content of the wheat gluten fraction. The same kind of calculation was performed considering that all exchangeable hydrogen atoms are replaced by deuterium (Figure S3). The mean SLD value shifts from  $(1.99 \pm 0.14)$  to  $(3.4 \pm 0.3) 10^{-6} \text{ \AA}^{-2}$ .

### 3. Incoherent background in SANS spectra

Incoherent background was estimated for each sample using a far-point method. A linear evolution of the incoherent background with sample deuteration was obtained (fig. S3). The incoherent background was subtracted to the sample spectra.

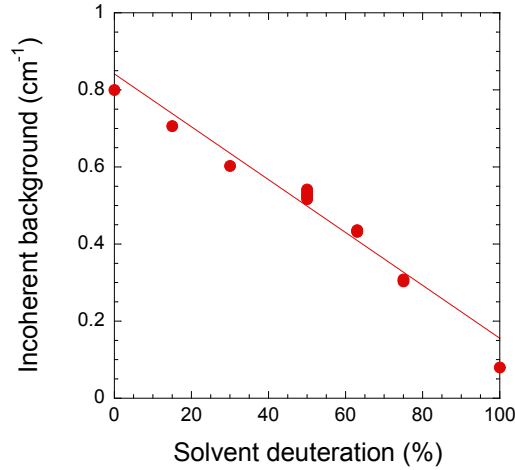


**Figure S3.** Evolution of the incoherent level in SANS spectra of D6 samples as function of the solvent deuteration determined according to the far point method.

### 4. Characteristic length scales in gluten gel samples

The two characteristic length scales,  $\xi$  and  $\bar{\mathcal{E}}$ , extracted from the fits with Eq. 1 and Eq. 2 (see main paper) are gathered in figure S4, for samples of the D6 group. We show in figure S4A the evolution of the large scale characteristic length,  $\bar{\mathcal{E}}$ , which can only be measured in the presence of a deuterated solvent. We mention that not all samples were measured on a very broad range of wave-vectors. For some samples (Series I'), data at small wave vectors are not available. Hence the plateau of the scattered intensity at small  $q$  is hardly measured and reliable measurements of the characteristic size  $\bar{\mathcal{E}}$  are not accessed. When  $\bar{\mathcal{E}}$  can be evaluated, we find that  $\bar{\mathcal{E}}$  is roughly constant ( $\bar{\mathcal{E}} = (600 \pm 100) \text{ \AA}$ ), independently on the samples investigated. Consequently, for the samples of Series I' the fit of the data using Eq. 2 are performed by imposing for  $\bar{\mathcal{E}}$  the average numerical value found experimentally for other samples.

On the other hand, reliable measurements of the blob size  $\xi$  are obtained for all samples. Figure S4B shows the evolution  $\xi$  with the solvent deuteration for samples of the D6 group. We find that  $\xi$  is constant ( $\xi = (15 \pm 5) \text{ \AA}$ ) for solvent deuteration up to 50% and steadily increases with solvent deuteration, reaching 30  $\text{\AA}$  for a fully deuterated solvent. The evolution of the blob size with solvent deuteration can be interpreted as resulting from an evolution of the protein flexibility. Indeed, for polymer chains in good solvent conditions, the scaling theory<sup>4</sup> predicts  $\xi = l_0 \Phi^{-3/4}$ , where  $l_0$  is the polymer persistence length, or monomer size for a flexible polymer, and  $\Phi$  is the volume fraction of polymer. Here  $\Phi = 0.18$ , yielding a persistence length that varies from 4 to 8  $\text{\AA}$  with solvent deuteration. These numerical values are in excellent agreement with our previous measurement for hydrogenated samples with various concentrations<sup>5</sup> and with the values experimentally found for unstructured proteins (between 5 and 7  $\text{\AA}$ )<sup>6</sup>. Note in addition that a stiffening of the protein chain with solvent deuteration has been measured by force spectroscopy for proteins similar to ours although simpler (model peptide of the repetitive domain of glutenins)<sup>7</sup>. Other studies have evidenced the influence of heavy water on the protein rigidity, with a rigidity that could increase<sup>8,9</sup> or decrease in the presence of  $\text{D}_2\text{O}$ <sup>9</sup> depending on the overall hydration of the proteins.

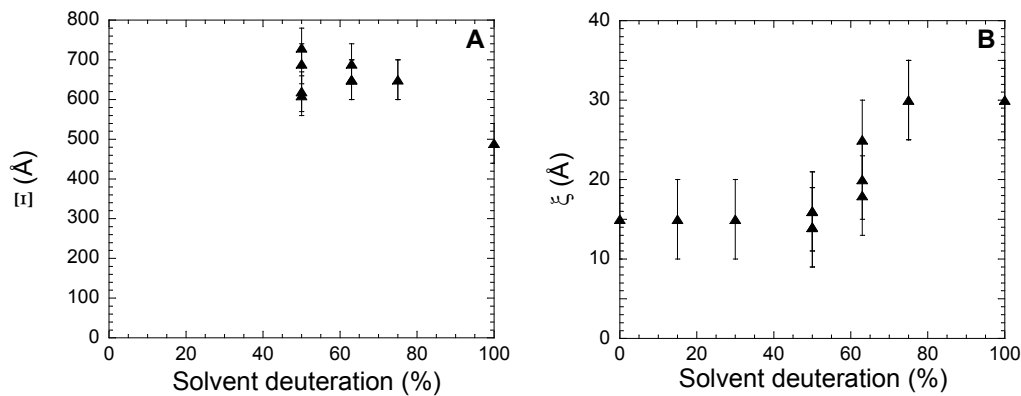


**Figure S4.** Large scale characteristic size  $E$  (A) and blob size  $\xi$  (B), as a function of the solvent deuteration for samples of the D6 group.

## 5. Contrast variations of Series II, III and IV

Using the same arguments as the one detailed in 3.3 in the main paper, one can explain the evolution of the amplitude of the scattering at large  $q$  for samples from Series II, III and IV (figures 4C, 4D, 4E). In these series the overall deuterium content is kept constant while the

origin of deuterium differs. Because water molecules contain 2 times more exchangeable deuteriums than ethanol molecules, the amount of labile deuterium varies along a series. Hence one expects a change of the SLD of the proteins, and consequently of the contrast  $(\bar{\rho}_{prot} - \rho_{solv})^2$ . We show in figure S5A, the evolution of  $\rho_{solv}$  and  $\bar{\rho}_{prot}$  (calculated as explained in 3.3) with the concentration of labile deuterium in the sample, and we show in figure S5B the evolutions of the intensity at  $q=10^{-1}\text{\AA}^{-1}$  as a function of the concentration of labile deuteriums in the samples. For samples of Series III and Series IV,  $\rho_{solv} > \bar{\rho}_{prot}$ . Hence as the amount of labile deuterium increases, the contrast decreases, as observed experimentally. By contrast, for samples of Series II,  $\rho_{solv}$  and  $\bar{\rho}_{prot}$  are expected to cross for a concentration of exchangeable D of about 45 mol/L. Consequently, one expects the contrast to vary in a non-monotonic fashion with the concentration of labile D, in full agreement with our experimental observations, although our data suggest a minimum contrast at a slightly lower concentration ( $\sim 30$  mol/L). On the other hand, comparable to samples of Series I and I' (see main paper) and non-zero values ( $I^0 \approx 0.03 \text{ cm}^{-1}$ ) are measured for the minimum contrast expected to be reached when  $\bar{\rho}_{prot} = \rho_{solv}$ .

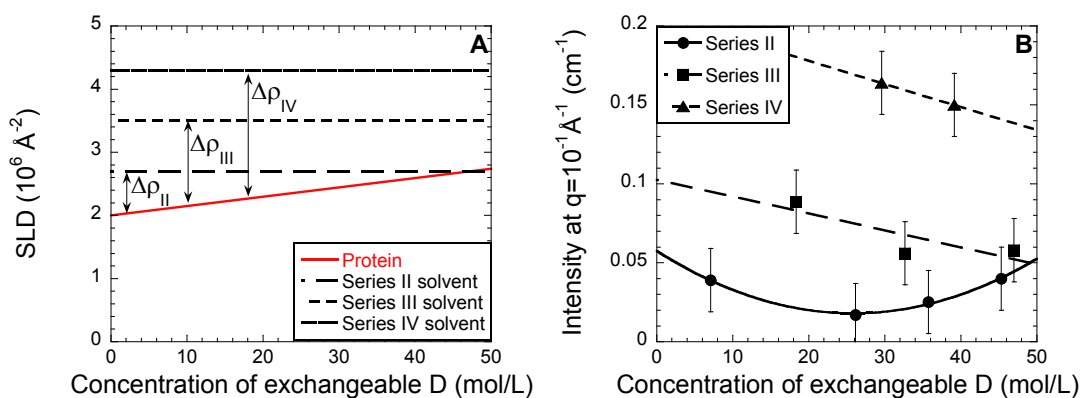


**Figure S5.** Intensities at  $q=10^{-1} \text{ \AA}^{-1}$  (B), and evolutions of the solvent and protein SLD (A) as a function of the concentration of labile deuterium. Lines in (B) are guides for the eyes.

4-

## References

1. M. H. Morel, P. Dehlon, J. C. Autran, J. P. Leygue and C. Bar-L'Helgouac'h, *Cereal Chem*, 2000, **77**, 685-691.

2. P. R. Shewry, D. Lafiandra, G. Salcedo, C. Aragoncillo, F. Garciaolmedo, E. J. L. Lew, M. D. Dietler and D. D. Kasarda, *Febs Lett*, 1984, **175**, 359-363.
3. B. Jacrot, *Rep Prog Phys*, 1976, **39**, 911-953.
4. P.G. de Gennes, *Scaling Concepts in Polymer Physics*, Ithaca and London, 1979.
5. M. Dahesh, A. Banc, A. Duri, M. H. Morel and L. Ramos, *J Phys Chem B*, 2014, **118**, 11065-11076.
6. T. Ohashi, S. D. Galiacy, G. Briscoe and H. P. Erickson, *Protein Sci*, 2007, **16**, 1429-1438.
7. S. J. Haward, P. R. Shewry, J. Marsh, M. J. Miles and T. J. McMaster, *Microsc Res Techniq*, 2011, **74**, 170-176.
8. P. Cioni and G. B. Strambini, *Biophys J*, 2002, **82**, 3246-3253.
9. M. Tehei, D. Madern, C. Pfister and G. Zaccai, *P Natl Acad Sci USA*, 2001, **98**, 14356-14361.